

Effective Components of *Panax notoginseng*–*Salvia miltiorrhiza* in the Treatment of Melasma and Its Experimental Study

Yunxia Wei, Xufeng Yu, Jing Zhao, Mingzhou Gao,* and Mingqi Qiao*



Cite This: *ACS Omega* 2025, 10, 3033–3043



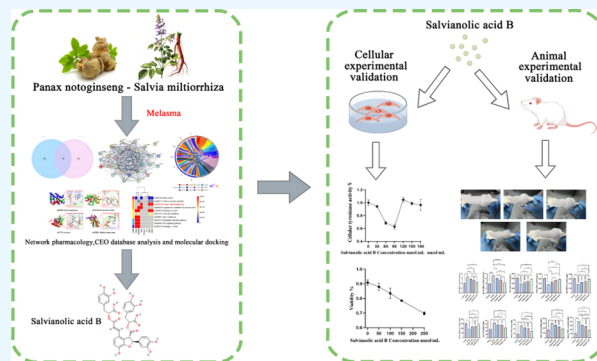
Read Online

ACCESS |

Metrics & More

Article Recommendations

ABSTRACT: Purpose: The main purpose of this study was to predict and verify the active ingredients of *Panax notoginseng*–*Salvia miltiorrhiza* in melasma based on network pharmacology analysis and experimental verification. Materials and methods: *Panax notoginseng*–*Salvia miltiorrhiza* was investigated by network pharmacology, GEO database analysis, and molecular docking techniques to screen its active ingredients. The active components of *Panax notoginseng*–*Salvia miltiorrhiza* were further validated by an in vitro α -melanin-induced B16F10 melanoma cell model and an in vivo UV irradiation combined with a progesterone injection-induced melasma rat model. Results: Network pharmacology analysis and molecular docking showed that salvianolic acid B might be the key active ingredient. In vitro cellular experiments revealed that salvianolic acid B inhibits tyrosinase activity in B16F10 cells at concentrations of 60–90 nmol/mL. In vivo animal experiments found that TYR, MDA, and TNF- α were decreased in the skin and serum of rats in the group of the low-, medium-, and high-dose groups of salvianolic acid B, and the expression of GSH-Px and SOD was increased. The high-dose groups of salvianolic acid B showed the best therapeutic effect. Conclusion: In this study, experiments collectively show that salvianolic acid B in *Panax notoginseng*–*Salvia miltiorrhiza* slows down the process of melasma by inhibiting lipid peroxidation in the organism, increasing the antioxidant capacity of the skin, decreasing the activity of tyrosinase, and providing anti-inflammation. This highlights the successful application of network pharmacology and provides a scientific basis for the clinical citation of *Panax notoginseng*–*Salvia miltiorrhiza* in treating melasma.



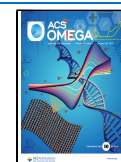
1. INTRODUCTION

Melasma is an acquired hyperpigmentation disorder characterized by increased levels of melanin production and deposition. It occurs most often in women of reproductive age and is one of the most common pigmentation disorders of the face.¹ Clinically, it presents as light to dark brown spots and plaques, and the common clinical examination tool is the Wood's lamp, which is classified into three main types according to the area of onset: central face, zygomatic bone involving the cheeks and nose, and mandible involving the jawline.^{2,3} Based on the location of pigmentation, melasma is a mixed epidermal–dermal hyperpigmentation, the etiology of which is thought to be caused by sex hormones with ultraviolet light exposure in a susceptible genetic background.^{3,4} Modern medical research has found a significant difference in blood rheology between patients with melasma and normal people, manifested by increased blood viscosity and slower blood flow in patients.⁵ The relationship between melasma and blood operation has also been documented in ancient Chinese medical texts, such as “Ling Shu, Meridian”, “If blood does not flow, the hair color is not glossy, so its face is as black as lacquer and firewood”; “Pujifang, The Gate of All Diseases of Women”, “The face is dull, which is caused by the clotting of

blood in the dirty”, and blood stasis is an important cause of melasma. *Panax notoginseng*–*Salvia miltiorrhiza* is a classic clinical compound formula for activating blood circulation and removing blood stasis, which plays a positive role in the treatment of melasma.

Chinese medicine pair refers to the basic form of Chinese medicine prescription by the theory of traditional Chinese medicine, which has been clinically applied for a long time and proven to be effective; it is the simplest way of Chinese medicine prescription and is the smallest compound prescription. *Panax notoginseng* is the dried root and rhizome of *Panax notoginseng*(Burk.) F.H. Chen of the family Wujiaceae, which is known to promote endothelial angiogenesis, alleviate chronic inflammation, and have antiviral effects.⁶ Studies have shown that total saponins of *Panax notoginseng* can improve

Received: October 29, 2024
Revised: December 21, 2024
Accepted: December 27, 2024
Published: January 14, 2025



vascular endothelial function, reduce blood viscosity, and inhibit platelet aggregation. *Salviae Miltiorrhizae Radix Rhizoma* is a traditional Chinese medicinal herb, which was first published in Shennong Ben Cao Jing (Classic of the Materia Medica of the Divine Husbandman), and modern pharmacological studies have concluded that *Salviae miltiorrhizae* has the effects of improving microcirculation, anticoagulation, antithrombosis, and antihypertensive.⁷ Its main components are water-soluble phenolic acids and fat-soluble tanshinones. Its dried roots and rhizomes are widely used to treat cardiovascular and cerebrovascular diseases in Asia, Europe, and the United States.⁸ It was found that when the two were combined, they were superior to those used alone in protecting vascular endothelial cells and inhibiting platelet adhesion and aggregation.⁹ In the present study, we used network pharmacology, GEO database analysis, molecular docking, and in vivo and in vitro experiments to investigate the active ingredients and related mechanisms of the *Panax notoginseng*–*Salviae miltiorrhizae* pairing for the treatment of melasma.

British pharmacologist Hopkins¹⁰ proposed the concept of “network pharmacology” in 2007 and defined it as a branch of pharmacology that utilizes a network approach to analyze the synergistic relationship between drugs and diseases and targets through “multi-components, multi-targets, and multi-pathways”. Network pharmacology has become a powerful means to study the active ingredients and active targets of traditional Chinese medicine.

With the maturity of gene chip technology and bioinformatics analysis methods, genome-wide screening analysis and validation are effective methods to discover diseases' molecular markers. Melasma-related data sets were downloaded from the GEO database to search for differentially expressed genes, and potential validated targets were explored for early diagnosis, targeted therapy, and prognostic analysis of melasma.¹¹

2. MATERIALS AND METHODS

2.1. Network Pharmacology. **2.1.1. Collection and Screening of Active Ingredients and Related Protein Targets of *Salviae miltiorrhizae* and *Panax notoginseng*.** The active ingredients of *Salviae miltiorrhizae* and *Panax notoginseng* were collected by searching the TCMSP database and SymMap database with the literature, and the retrieved data were screened with an index of DL \geq 0.18. Drug likeness (DL) refers to the similarity of compound components to known drugs. Using the obtained active ingredients, the protein target information corresponding to each active ingredient was collected and organized by searching the database.

For subsequent research, the protein targets obtained above need to be standardized and converted by entering the protein target information into the UniProt database, setting the filtering condition of species as “Homo Sapiens”, eliminating unvalidated targets, and then finally obtaining the names of the target genes of the drug action (gene symbol).

2.1.2. Acquisition of Melasma Disease Gene Targets and Integration of Intersecting Genes. Using “melanosis” as the keyword, GeneCardsrds (<https://www.genecards.org>) and DisGeNET databases (<https://www.disgenet.org/>) were searched for melasma-related gene targets. All the search results were exported, and summarized and duplicated data were eliminated using the software Excel, and the gene-related target information on melasma was finally obtained. To

visualize the correlation between the active ingredients of TCM and the gene targets of melasma, the Venny2.1 tool was used to take the intersection of the two targets with each other, to derive the potential targets of TCM for the treatment of melasma, and to draw a “drug-disease” Wayne diagram.

2.1.3. Protein Interaction Network Construction. To obtain the core key targets, the intersection targets obtained above were inputted into the STRING database (<https://cn.string-db.org/>, Version 11.5) for searching. The condition type was set as *Homo sapiens*, and the analysis mode as multiple proteins. “confidence” (>0.4) was used as the standard, eliminating the nodes that are not connected, outputting the image, and saving it after getting the results to obtain the final protein interaction network (PPI).

2.1.4. GEO Database Screening for Core Differential Genes. The GEO database (<https://www.ncbi.nlm.nih.gov/geo/>) was utilized to search for “meloidosis”, and the data set GSE72140 was downloaded by reading the literature. The data were subjected to GEO2R ($p < 0.05$, $|\log\text{FC}| > 0.5$) to obtain differential genes.

2.1.5. GO Functional Enrichment Analysis and KEGG Pathway Enrichment Analysis. GO enrichment analysis is the process of finding a collection of genes with a particular function by using the significant correlation between a set of known or hypothetical genes and GO annotations (by definition, a highly specific structural classification system), and it is an important means of studying the relationship between gene expression profiles and functions. Genes are usually categorized into biological process (BP), cellular component (CC), and molecular function (MF).¹² The KEGG database is a comprehensive bioinformatics database established in 1995 by the Kanehisa Laboratory at the Center for Bioinformatics, Kyoto University, Japan. KEGG enrichment analysis is a bioinformatics technique that utilizes the information in the KEGG database to enrich experimental data for the detection of genes related to the KEGG pathway in the set of genes under investigation. KEGG enrichment analysis reveals not only the gene relationships present in the collection of related genes but also the differences in the positions of gene involvement.

GO and KEGG enrichment analyses were performed on the above-obtained intersecting targets with R4.2.2 to obtain the enriched biological processes, cellular components, molecular functions, and signaling pathway information using the conditioned species as *Homo sapiens*, and to obtain GO-BP enrichment analysis chordal maps and KEGG enrichment analysis heat maps.

2.2. Molecular Docking. First, the 2D structure of the core component was obtained by using the PubChem platform, optimized by Chem3D software, and saved in the format with the suffix mol2. The 3D structure of the core target was also obtained through the RCSBPDB (<https://www.genecards.org>) platform, then imported into PyMOL software, optimized by removing water molecules and irrelevant small molecules, and saved in the format of suffix pdb. The obtained file was calculated by AutoDock Vina1.1.2 software to molecularly dock the target structure with the core active ingredient structure in the mode of minimum binding energy; then the docking results were imported into PyMOL3.0 software for plotting to process; and finally, the molecularly docked binding pattern diagram was output.

2.3. Experimental Validation. **2.3.1. Cells and Cell Culture.** Under aseptic conditions, B16F10 mouse melanoma

Table 1. Prediction of Targets for Melasma Treatment by *Panax notoginseng*–*Salviae miltiorrhizae*

Targets				
EIF6	NR3C2	TNF	PGR	CDK2
TYR	CYP3A4	IL6	PTGS2	EGF
IKBK	CDKN1A	CCL2	ESR1	NOS2
MET	MAPK8	CXCL8	CCND1	HRAS
EDN1	PCNA	PTEN	CDK6	
CSF2	IL1B	ESR2	PRKACA	

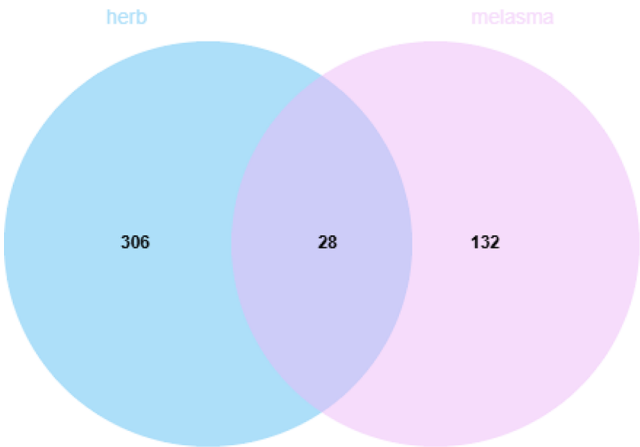


Figure 1. Venn diagram of *Panax notoginseng*–*Salviae miltiorrhizae* worked targets and melasma-related genes.

cells (purchased from Xuzhou Doli Biotechnology Limited Company) were inoculated in RPMI-1640 medium (Punosai, Hubei, China) containing 10% fetal bovine serum (Vivacell, Shanghai, China) and 1% triple antibody (Vivacell, Shanghai, China), and cultured in a CO₂ incubator (Shanghai Lixin Scientific Instrument Limited Company, Shanghai, China) at

Table 2. Results of GEO Database Screening for Differentially Expressed Genes

Targets	log FC
ESR1	0.9162920
TYR	0.8519693
PGR	0.7746751
ESR2	0.7669158
PTEN	−0.6377178
CYP3A4	−0.5641005
MAPK8	0.5029076

37 °C, 5% CO₂, and 98% relative humidity. The fresh culture medium was changed once a day.

2.3.2. Cell Viability. When the cells grow to 80–90% fusion state, 2 mL p.p.b. is added, the dish is rinsed, and the dish is slightly shaken, followed by cell infiltration for 30–60 s. The cells are digested with 1 mL of 0.25% trypsin (Vivacell, Shanghai, China) for 2–5 min, then 2 mL of basal medium is added to terminate the digestion. The inner wall of the dish is rinsed with complete medium, so that the cells are completely dislodged and mixed uniformly. The single-cell suspension is put into a 15-mL centrifuge tube, centrifuged for 5–10 min, the excess waste liquid is poured off, and complete medium is added to prepare a single-cell suspension. Ten microliters of single-cell suspension is taken and counted by a cell counting plate, and the concentration of cells is adjusted to 1 × 10⁵ cells/mL by using the fresh medium. The cells are inoculated into a 96-well culture plate, 100 μL per well, and cultured in a CO₂ incubator for 24 h. After the cells are attached to the wall, the supernatant is discarded, rinsed once with PBS, and 100 μL of fresh culture medium containing different concentrations of salvianolic acid B (Chengdu Mansion Biotechnology Limited Company, Sichuan, China) is added (salvianolic acid B concentrations of 50, 100, 150, and 250 μg/mL, 6 replicate wells are set up in each group, and the corresponding drug is

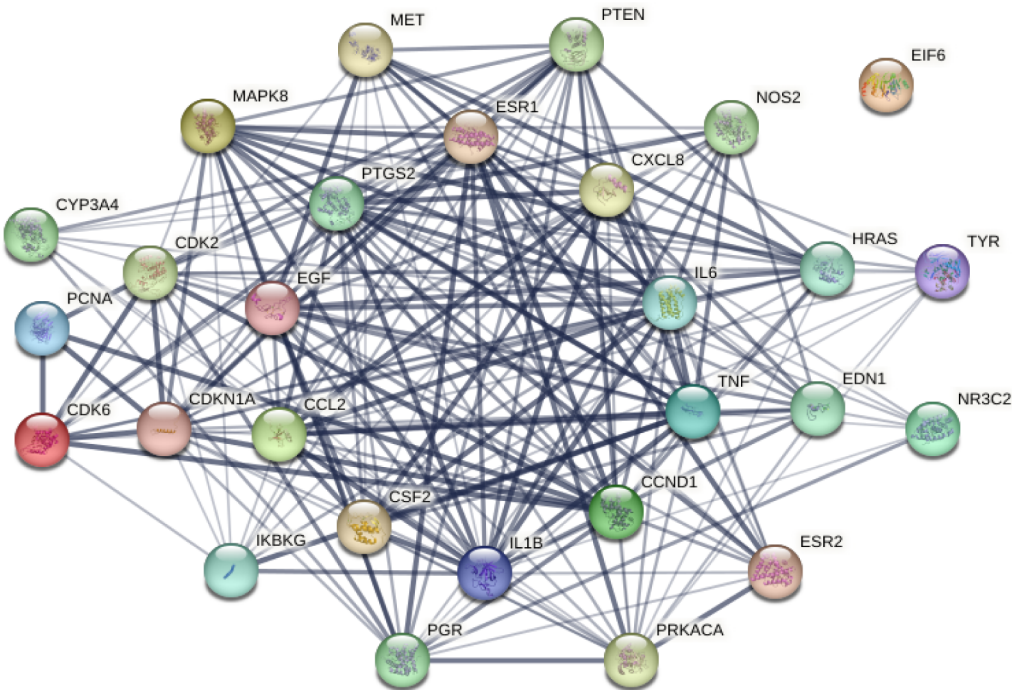


Figure 2. PPI network analysis of 28 potential targets.

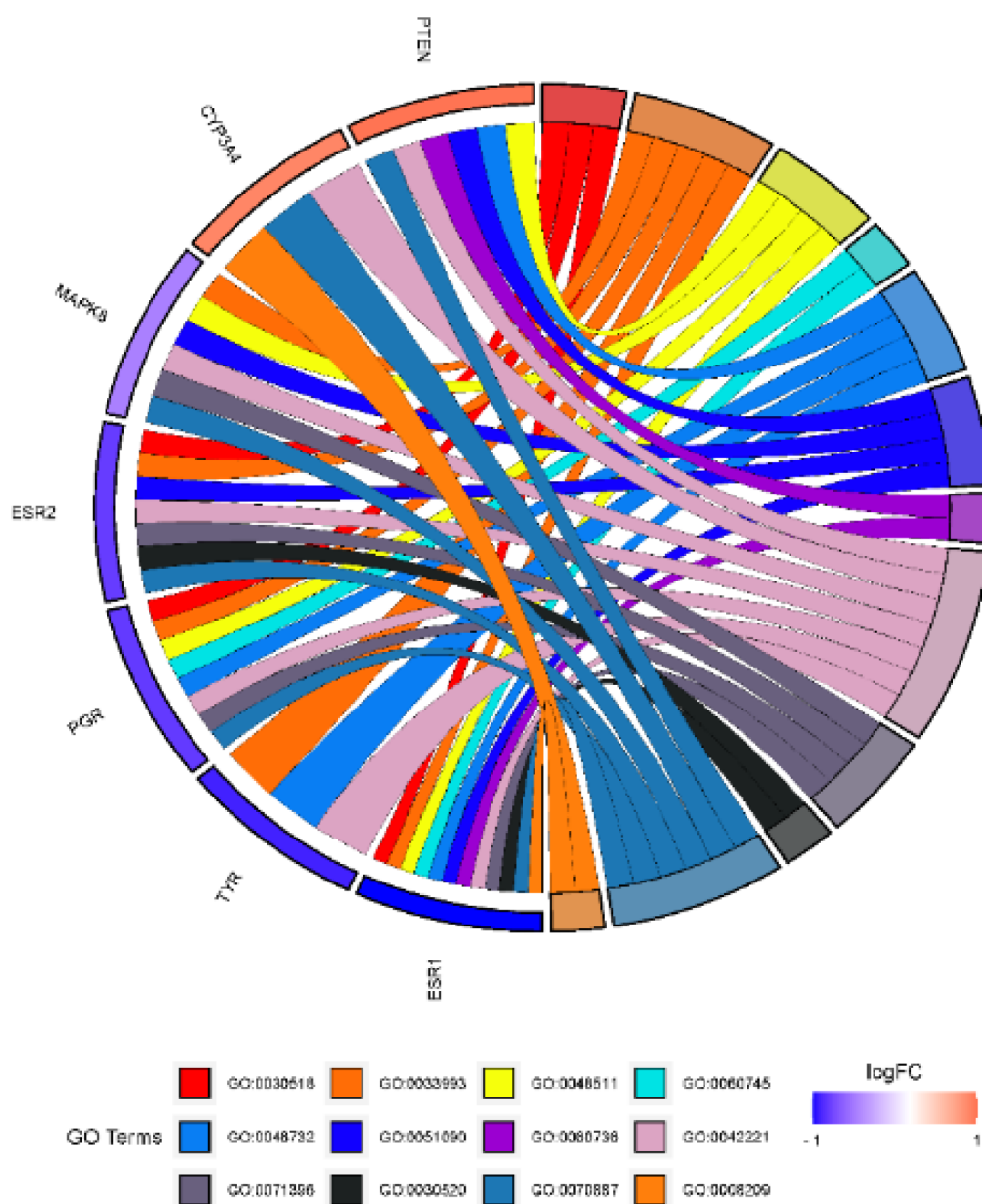


Figure 3. GO enrichment of 7 potential targets.

added to treat the cells for 24 h). The background control group is set up, which is the background without cells, and only the medium is added. The supernatant was aspirated, 100 μ l of CCK-8(CCK-8:1640 = 1:10) solution was added, and the cells were incubated in the incubator for 1–4 h. The optical density (OD) at 450 nm was measured by an enzyme marker, and the cell viability rate was calculated as $[(\text{OD drug administration group} - \text{OD background control group}) / (\text{OD model group} - \text{OD background control group})] \times 100\%$.

2.3.3. Determination of Intracellular Tyrosinase Activity. Cells were treated as described in section 2.3.2. After 24 h of incubation, the supernatant was discarded, 90 μ L of PBS buffer containing 1% TritonX-100 (Bioss, Beijing, China) was added to each well, and 10 μ L of 1 mg/mL levodopa (L-DOPA) (Solebo, Beijing, China) was added. The cells were incubated at 37 °C for 60 min, and the OD value of each well at 490 nm was detected by an enzyme marker. 37 °C incubation for 60 min, and then the OD value of each well at 490 nm was

detected by an enzyme marker. The intracellular tyrosinase activity was calculated using the formula: Tyrosinase activity = $(\text{test well OD}_{490 \text{ nm}} - \text{blank well OD}_{490 \text{ nm}}) / (\text{control well OD}_{490 \text{ nm}} - \text{blank well OD}_{490 \text{ nm}})$.

2.3.4. Animal Experiment. SPF-grade healthy female SD rats (purchased from Viton Lever Biotechnology Limited Company, Beijing, China), 30 rats, body mass (180 ± 20) g, 8 weeks old, License No.: SCXK (Beijing) 2021–0006, were housed in the SPF-grade animal room of the Shandong University of Traditional Chinese Medicine. During the experimental period, the rats were free to drink water, room temperature: 20–22 °C, relative humidity: 60–70%, with a 12 h/12 h day/night alternation. The rats were kept in three cages. After 1 week of adaptive feeding, 30 rats were randomly divided into 5 groups: blank group, model group, and low-, medium-, and high-dose groups of salivianolic acid B (low-, medium-, and high-dose groups were 5, 7, and 9 mg/mL salivianolic acid B), with 6 rats in each group. The skin of the

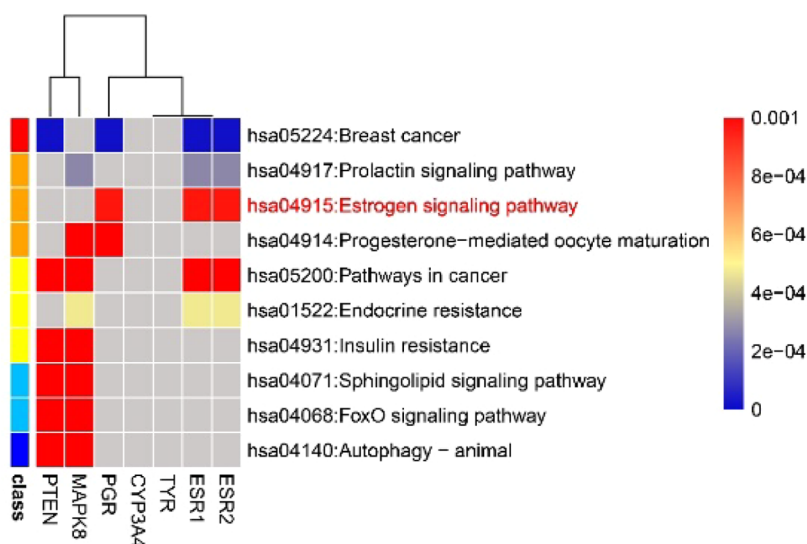


Figure 4. KEGG pathway enrichment of 7 potential targets.

back of the rats was depilated (3×3 cm). UV (Philips, Germany) with a wavelength of 320 nm, 15 W, was selected. Local irradiation of the skin was carried out once a day for 60 min each time. The distance between the skin of the rats and the light source was 10–15 cm, and irradiation was carried out continuously for 42 days. In addition to the blank group, the rats in the rest of the groups were irradiated by UVB in the morning combined with the intramuscular injection of progesterone 7.5 mg/kg, once a day, for 7 days, rested for 1 day, and were irradiated continuously for 42 days, and a rat melasma model was prepared. The blank group and the model group were given a saline coating, and the rest of the groups were given (5, 7, and 9 mg/mL salivianolic acid B) of the corresponding drugs, modeling in the morning, and the tested drugs in the afternoon. On the 42nd day of the experiment, the skin changes on the back of the rats were observed, such as the color of the skin lesions, the color depth of the patches, the size of the patches, and photographs were taken and recorded. Then, the rats were respiratorily anesthetized, and after they were completely unconscious, their limbs were unfolded with binding wires, and their heads and bodies were kept flat and tied to the rat boards for blood sampling from the abdominal aorta. The blood from the abdominal main artery was centrifuged with a low-temperature centrifuge (4°C) at 3500 rpm for 15 min, and then the upper layer of the blood serum was sucked up by a pipet gun to use it as an index for testing. After the blood was sampled from the rat, the skin of the irradiated part was cut off with scissors from its back by $1\text{ cm} \times 1\text{ cm}$. The skin of the irradiated area was saline-plated. After blood sampling, rats were cut $1\text{ cm} \times 1\text{ cm}$ from the irradiated area on the back with clippers, rinsed with saline, and put into EP tubes.

3. RESULTS

3.1. Targets Related to the Treatment of Melasma by *Panax notoginseng*–*Salviae miltiorrhizae*. A total of 160 melasma-related targets were screened from the GeneCards and Disgenet databases. Next, 28 common targets were obtained from 334 *Panax notoginseng*–*Salviae miltiorrhizae* potential targets and 160 melasma-related genes (Table 1 and Figure 1).

3.2. PPI Protein Network Analysis. Protein interaction analysis (<https://string-db.org/>) was performed on cross-targets using the STRING database to obtain a plot of potential target interactions, as shown in Figure 2, where EIF6 did not interact with other targets and was therefore removed.

3.3. GEO Database. Through the GEO database, we obtained each gene chip from the GSE72140 data set, and a total of 7 target genes were obtained from the differential genes analyzed by GEO2R online with $p < 0.05$, $|\log \text{FC}| > 0.5$, and the intersection was taken to target genes with 3.2, as shown in Table 2. Among them, PTEN and CYP3A4 were down-regulated genes, and ESR1, TYR, PGR, ESR2, and MAPK8 were up-regulated genes.

3.4. GO Enrichment and KEGG Pathway Enrichment Analysis. In order to analyze the signaling pathways and possible functional roles of the differential genes, GO functional enrichment analysis ($p < 0.05$) and KEGG signaling pathway enrichment analysis ($p < 0.05$) were performed on the common targets. The enrichment results were analyzed in R language, and the GO enrichment analyses are shown in Figures 3 and 4. The GO functional enrichment analyses revealed that the therapeutic mechanisms may involve hormone metabolism, lipid metabolism, and transcription factor regulation in biological processes. Melasma is most commonly found in the center of the face, where sebaceous glands are dense. Keratin-forming cells, which produce and secrete large quantities of glucose ceramides and sphingomyelin precursors into the extracellular structural domains of the stratum corneum, constitute the epidermal barrier, and melasma is seen as a compromised skin barrier. Lipid metabolism may be associated with the pathogenesis of melasma.¹³ Figure 4 shows the KEGG signaling pathway analysis, where we mark in red the pathway with the highest association with melasma. According to the KEGG signaling pathway analysis, the estrogen signaling pathway may be associated with the treatment of melasma.

3.5. Molecular Docking Analysis. The results are shown in Table 3. Among them, cryptotanshinone has the smallest binding energy to protein receptors. The main chemical components of *Panax notoginseng* are saponins.¹⁴ *Salvia miltiorrhiza*'s main components are water-soluble phenolic acids as well as fat-soluble tanshinones.¹⁵ TYR is a key target

Table 3. Molecular Docking Results of *Panax notoginseng*–*Salvia miltiorrhiza* Components with 7 Potential Targets

PubChem CID	Compounds	Targets	Affinity (kcal/mol)	PDB ID	UniProt ID
160254	Cryptotanshinone	PGR	−10.3	1A28	P06401
6451084	Salvianolic acid B	TYR	−9.992	4QBT	P54577
14609851	4-Methylenemiltirone	ESR1	−9.817	1X7R	P03372
80970	Methylrosmarinat	ESR1	−9.761	5TMU	P03372
44425166	Isotanshinone II	ESR1	−9.735	5DTV	P03372
5320066	Neocryptotanshinone ii	ESR1	−9.679	4IV2	P03372
5319836	Miltionone II	PGR	−9.661	1SR7	P06401
14139388	Przewalskin	ESR1	−9.647	1ZKY	P03372
5742590	Sitogluside	PGR	−9.637	3K22	P04150
3082765	Dehydromiltirone	ESR1	−9.57	4IV2	P03372
10086184	Miltipolone	ESR1	−9.534	1ZKY	P03372
3083515	Danshenol B	PGR	−9.46	1SR7	P06401
44425166	Isotanshinone II	ESR2	−9.409	2GIU	Q92731
135872	2-Isopropyl-8-methylphenanthrene-3,4-dione	ESR1	−9.337	1X7R	P03372
89406	Dihydroisotanshinone I	ESR1	−9.31	3HLV	P03372
5280863	Kaempferol	PGR	−9.23	3GDH	Q96RS0
128994	Dehydrotanshinone II A	ESR1	−9.215	3HLV	P03372
5280863	Kaempferol	MAPK8	−9.123	3V3V	P45983
5320113	Dan-shexinkum b	ESR1	−9.114	4IV2	P03372
160142	Miltirone	ESR1	−9.092	4IV2	P03372
5280445	Luteolin	TYR	−9.081	6LN1	Q13627
15690458	Deoxyneocryptotanshinone	ESR1	−8.869	4IV2	P03372
64945	Ursolic acid	MAPK8	−8.617	4HYS	P45983
5280343	Quercetin	CYP3A4	−8.553	1OG5	P11712
5280666	Chryseriol	ESR1	−8.513	1X7R	P03372
5319835	Miltionone I	ESR1	−8.507	4IV2	P03372
164676	Tanshinone iia	CYP3A4	−8.443	5A1R	P08684
114829	DFV	ESR1	−8.34	1X7R	P03372
102004791	Epidanshenspiroketallactone	ESR1	−8.18	5KR9	P03372
5281654	Isorhamnetin	ESR1	−8.148	1X7R	P03372
129716399	8-Isopentenyl-kaempferol	ESR1	−8.089	1X7R	P03372
16102114	Przewalskin b	PGR	−7.856	1E3K	P06401
5280863	Kaempferol	CYP3A4	−7.843	1OG5	P11712
14985	VIV	ESR1	−7.799	7N9O	P03372
9841799	(2R)-3-(3,4-Dihydroxyphenyl)-2-[(Z)-3-(3,4-dihydroxyphenyl)acryloyl]oxy-propionic acid	ESR1	−7.693	7RS7	P03372
5320113	Dan-shexinkum b	ESR2	−7.641	2GIU	Q92731
5280343	Quercetin	PTEN	−7.615	1D5R	P60484
5281654	Isorhamnetin	ESR2	−7.542	1X7J	Q92731
12303645	Sitosterol	PGR	−7.267	3D90	P06401
5280794	Stigmasterol	PGR	−7.264	1REM	P61626
105119	1,2-DT-quinone	ESR1	−7.165	4PXM	P03372
14609850	(4bS,8aS,10S)-10-Hydroxy-2-isopropyl-4b,8,8-trimethyl-5,6,7,8a,9,10-hexahydrophenanthrene-3,4-dione	PGR	−7.131	3GDH	Q96RS0
5281702	Tricin	ESR2	−7.114	1X7J	Q92731
5281330	Poriferasterol	PGR	−7.033	1E3K	P06401
5281702	Tricin	ESR1	−6.8	2QE4	P03372
222284	β -Sitosterol	PGR	−6.308	1E3K	P06401
6709746	2-(4-Hydroxy-3-methoxyphen)-5-(3-hydroxypropyl)-7-methoxy-3-benzofurancarboxaldehyde	ESR2	−6.179	1U9E	Q92731
6709746	2-(4-Hydroxy-3-methoxyphenyl)-5-(3-hydroxypropyl)-7-methoxy-3-benzofurancarboxaldehyde	ESR1	−5.782	1X7E	P03372
457801	Poriferast-5-en-3beta-ol	PGR	−5.445	1E3K	P06401

for tyrosinase synthesis. Therefore, combined with the magnitude of molecular binding energy, we chose cryptotanshinone, salvianolic acid B, luteolin, and methylrosmarinat for PyMOL visualization, as shown in Figure 5, where the active ingredient is shown in white, the protein receptor binding region is shown in orange, and the intermolecular hydrogen bonds are marked with green-dashed lines. Through Figure 5,

it was found that methylrosmarinat was unstable to bind to ESR1 through the Π bond; therefore, we concluded that methylrosmarinat might not be the main effector component of *Panax notoginseng*–*Salvia miltiorrhiza* for melasma. Some studies showed that tanshinones did not have significant inhibitory effects on tyrosinase and that salvianolic acid B might be the main effector component for melasma treatment.

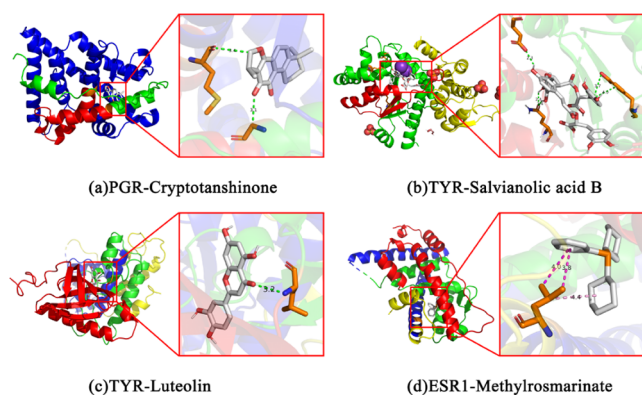


Figure 5. Molecular docking of cryptotanshinone to PGR (a), salvianolic acid B to TYR (b), Luteolin to TYR (c), and methylrosmarinate to ESR1 (d).

3.6. Experimental Validation. **3.6.1. Salvianolic Acid B Inhibits α -MSH-Induced Tyrosinase Synthesis in B16F10 Mouse Melanoma Cells.** Data from the CCK8 assay showed dose-dependent inhibition of melanoma cell activity in B16F10 mice by salvianolic acid B in the 50–250 nmol/mL range, as shown in Figure 6. The dose of salvianolic acid B, which had

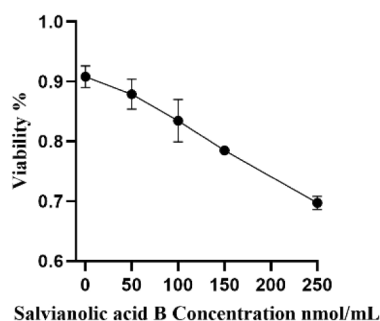


Figure 6. Effect of different concentrations of salvianolic acid B on the cell proliferation rate.

no significant effect on the activity of B16F10 mouse melanoma cells, was selected to treat the cells for 24 h. 300 nmol/L- α -MSH was added to each group, the enzyme labeling instrument detected the content of intracellular tyrosinase, and the results are shown in Figure 7. The activities of intracellular tyrosinase were reduced by 20.69% at the test concentrations of 60 nmol/mL and 16.42% at 90 nmol/mL, respectively. Salvianolic acid B had an inhibitory effect on the

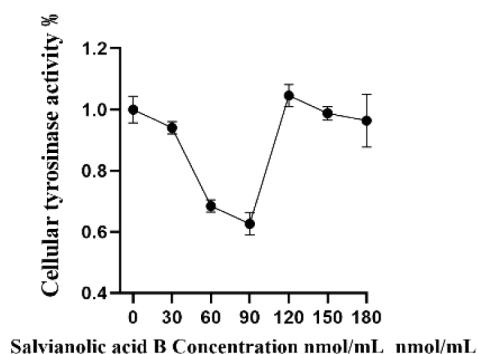


Figure 7. Effect of different concentrations of salvianolic acid on tyrosinase activity.

activity of intracellular tyrosinase in B16F10 cells at concentrations of 60–90 nmol/mL.

3.6.2. Salvianolic Acid B Ameliorates Ultraviolet Light Combined with Progesterone-Induced Melasma in a Rat Model. A model of UV irradiation combined with progesterone-induced melasma in rats was established, and the apparent skin status of the rats in each group was observed, as shown in Figure 8. The back skin of the rats in the model group showed

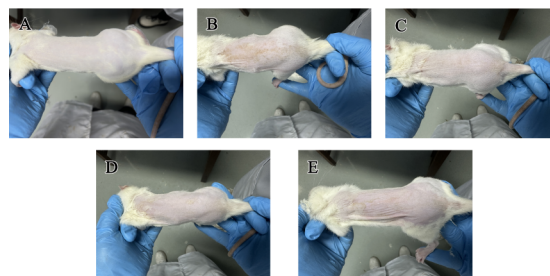


Figure 8. Apparent skin changes in rats (note: A: control group; B: model group; C, D, and E: low, medium, and high dose treatment groups of salvianolic acid B, respectively).

obvious yellow spots, while the irradiated skin of the rats in each dose group of salvianolic acid B showed only slight yellow spots, and there was no thickening of the skin, desquamation, or blisters. The levels of TYR, SOD, MDA, GSH-Px, and TNF- α in the skin and serum of rats in each group were detected by the enzyme-linked immunosorbent assay (ELISA), as shown in Figure 9. The levels of TYR activity, MDA, and TNF- α in the skin and serum of rats in the model group were significantly higher, and the activities of GSH-Px and SOD were significantly lower, while the levels of TYR, MDA, and TNF- α in the skin and serum of rats in the low-, medium-, and high-dose groups of salvianolic acid B were lower, and the expressions of GSH-Px and SOD were increased.

4. DISCUSSION

Melasma is clinically difficult to treat and prone to recurrence, which brings great mental and psychological pressure to patients. There is no clear treatment method; hydroquinone monotherapy and triple cream are the most commonly used methods for treating melasma, but they can induce adverse reactions such as skin irritation, dryness, and burning.¹⁶ The overactivity of melanocytes and increased tyrosinase synthesis are the main reasons for the development of melasma. The advantages of TCM in intervening in tyrosinase synthesis and maintaining the homeostasis of the body's internal environment are becoming more and more prominent. A series of studies have shown that melasma patients have high blood viscosity, which provides a solid foundation for the theory of "no stasis, no spot" in Chinese medicine. The study of *Panax notoginseng*–*Salvia miltiorrhiza*, a pair of medicines commonly used to activate blood circulation and eliminate blood stasis in the clinic, has yet to be finalized in terms of the active ingredients and the mechanism of its treatment of melasma.

In this study, 334 potential targets of *Panax notoginseng*–*Salviae miltiorrhizae* were predicted. PTEN, CYP3A4, ESR1, TYR, PGR, ESR2, and MAPK8 were identified as the key targets by PPI network and GEO database analysis. Melasma pathogenesis was found to be related to the estrogen signaling pathway by KEGG analysis, which involves the expression of PGR, ESR1, and ESR2.

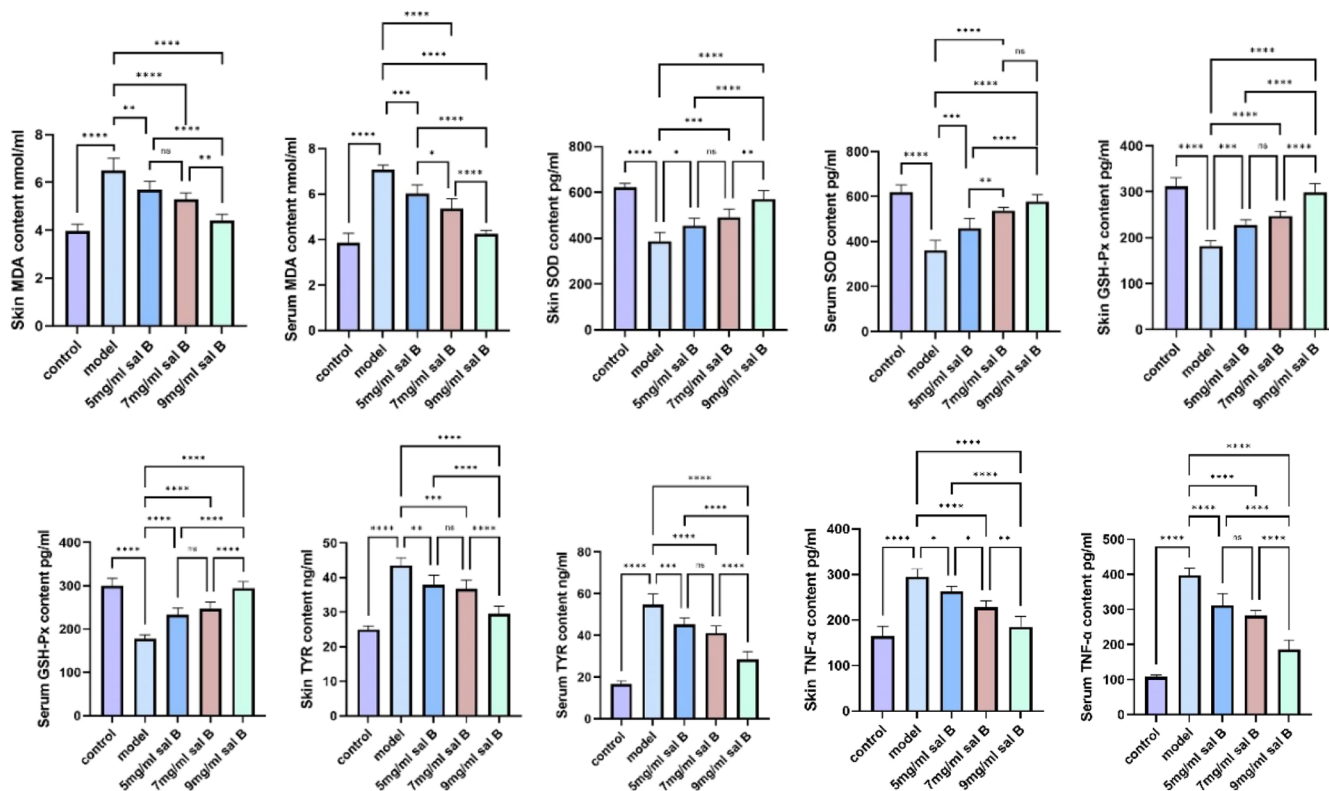


Figure 9. Detection of MDA, SOD, GSH-Px, TYR, and TNF- α in serum and skin tissues of rats (* $p < 0.05$ ** $p < 0.01$ *** $p < 0.001$ **** $p < 0.0001$).

The progesterone receptor (PGR) belongs to the nuclear transactivator superfamily of factors that can play an important role in binding to progesterone, a steroid hormone synthesized by the placenta, ovary, and adrenal glands.¹⁷ Progesterone receptors have an important interrelationship with estrogen receptors and regulate biological responses together. The progesterone receptor inhibits estradiol-induced estrogen receptor activity.¹⁸ A series of studies have shown that estrogen and progesterone are associated with the development of melasma. Estrogen induces the synthesis of melanogenic enzymes such as tyrosinase, TRP-1, TRP-2, and MITF, which in turn promotes melanogenesis,¹⁹ whereas progesterone inhibits estrogen-induced melanocyte activity, but its regulatory pathway does not depend on inhibition of tyrosinase activity.²⁰ Therefore, combined with the bioinformatics analysis, we believe that *Panax notoginseng*–*Salviae miltiorrhizae* may regulate the estrogen signaling pathway through multicomponents, thus inhibiting the bioactivity of melanocytes to improve melasma. Still, the regulatory pathway needs further research and validation.

After that, we molecularly docked the key target with the active ingredient and identified its core component, salvianolic acid B. Therefore, we hypothesized that *Panax notoginseng*–*Salviae miltiorrhizae*'s therapeutic mechanism might be related to salvianolic acid B.

Salvianolic acid B is the main water-soluble phenolic acid component of *Salvia miltiorrhiza*, which is condensed from phenylpropanoid structures and has good biological activity. A series of studies have found that salvianolic acid B has high antioxidant activity. Wang et al. found that salvianolic acid B could attenuate oxidative stress-induced injury by regulating the Akt/GSK3 β signaling pathway and further ameliorated

H₂O₂-induced intestinal epithelial barrier dysfunction and mitochondrial dysfunction.²¹ Yifan et al. found that salvianolic acid B protects against cystine-induced oxidative damage in vitro and in vivo.²² Lin et al. found that salvianolic acid B modulates the Nrf2 signaling pathway to reduce cisplatin-induced apoptosis and oxidative stress.²³ In addition, some studies found that salvianolic acid B has better anti-inflammatory activity, and salvianolic acid B can significantly reduce the overexpression of TNF- α and iNOS and inhibit the related inflammatory responses in the rat model of thrombotic occlusive vasculitis induced by sodium laurate.²⁴ Zhao et al. found that salvianolic acid B may reduce cell death and oxidative stress induced by cisplatin through the modulation of the NF- κ B/NLRP3 pathway to inhibit atherosclerosis and inflammatory responses.²⁵ A series of studies have shown that UV radiation is a major factor that induces and exacerbates melasma. Its pathogenic mechanism involves melanin metabolism, oxidative stress, etc. UV radiation induces the production of reactive oxygen species (ROS). Superoxide dismutase combines with ROS to produce hydrogen peroxide, which is further decomposed into harmless water by GSH-Px,²⁶ and oxidative stress occurs when the reactive oxygen species content exceeds the body's limitation and the imbalance of the body's antioxidant system.²⁷ Then, ROS will activate the MAPK signaling pathway and the NF- κ B signaling pathway. Receptor tyrosine kinase-ROS interactions of the MAPK signaling pathway activate Ras proteins, which in turn activate B-Raf kinase, which in turn activates ERK, JNK, or p38, and activation of ERK or JNK leads to the synthesis of MITF, which subsequently up-regulates melanogenesis-associated proteins and promotes melanin synthesis, or may increase the production of MITF through the NF- κ B signaling

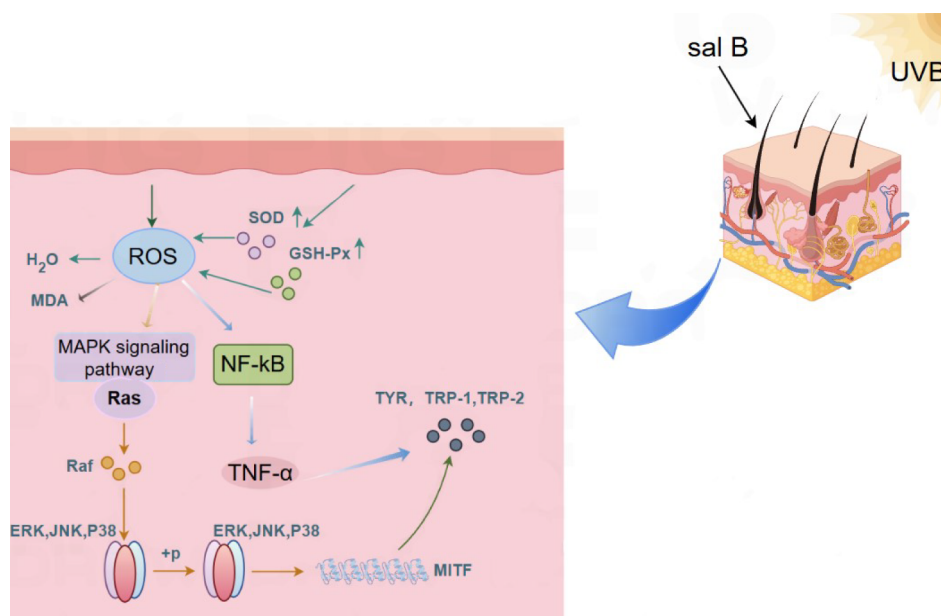


Figure 10. Therapeutic mechanism of salvianolic acid B diagram (salvianolic acid B may inhibit melanin synthesis by increasing the activity of SOD and GSH-Px, reducing the production of ROS, modulating the MAPK signaling pathway to reduce the activity of ERK, JNK, or p38, and down-regulating the expression of MITF, or modulating the NF- κ B signaling pathway to down-regulate the expression of pro-inflammatory cytokines, such as TNF- α , to regulate inflammatory responses, which may inhibit the activity of melanocytes and decrease the melanin synthesis).

pathway increases the expression of pro-inflammatory cytokines such as TNF- α , which modulates the inflammatory response and activates melanocytes.²⁸ Therefore, we hypothesized that salvianolic acid B may improve melasma by increasing the body's antioxidant capacity and inhibiting the inflammatory response.

Given the above predictions, we produced a B16F10 melanoma cell model and a melasma SD rat model for preliminary validation. We observed the effects of salvianolic acid B on the tyrosinase activity and cell proliferation of B16F10 melanoma cells to determine the therapeutic efficacy. The results demonstrated that salvianolic acid B had an inhibitory effect on the expression of tyrosinase activity within the range of 60–90 nmol/mL and that salvianolic acid B had an effect on the expression of tyrosinase activity in a dose-dependent manner. The molecular mechanism of melasma treatment with salvianolic acid B was further elucidated by detecting the melasma markers SOD, GSH-Px, TYR, MDA, and TNF- α . The results showed that the model group triggered oxidative stress and inflammatory response with lower expression of SOD and GSH-Px and higher expression of MDA and TNF- α , while the expression of these signaling molecules was inhibited in the group of salvianolic acid B administration. Therefore, salvianolic acid B could inhibit the inflammatory response of the organism and restore the balance of the human body's antioxidant system to achieve the effect of treating melasma, as shown in Figure 10.

In summary, based on the collective data from network pharmacology, GEO database analysis, and molecular docking analysis, we proposed that salvianolic acid B is the key active ingredient of *Panax notoginseng*–*Salviae miltiorrhizae* involved in the treatment of melasma and that its molecular mechanism involves oxidative stress and inflammatory response, and further verified our hypothesis in vivo and in vitro. According to the KEGG pathway analysis, the estrogen signaling pathway is closely related to the development of melasma, and estrogen

induces melanin synthesis, while progesterone can inhibit estrogen-induced melanocyte activity. Salvianolic acid B may regulate the estrogen signaling pathway through the regulation of PGR expression, thus affecting melanogenesis and improving melasma in patients. The detailed molecular mechanism will be further explored in future studies.

AUTHOR INFORMATION

Corresponding Authors

Mingzhou Gao – Innovation Research Institute of Traditional Chinese Medicine, Shandong University of Traditional Chinese Medicine, Jinan 250355, China;
Email: gmingzhou@163.com

Mingqi Qiao – Innovation Research Institute of Traditional Chinese Medicine, Shandong University of Traditional Chinese Medicine, Jinan 250355, China; orcid.org/0009-0007-8665-4054; Email: qmingqi@163.com

Authors

Yunxia Wei – Shandong University of Traditional Chinese Medicine, Jinan 250355, China

Xufeng Yu – Shandong University of Traditional Chinese Medicine, Jinan 250355, China

Jing Zhao – Shandong University of Traditional Chinese Medicine, Jinan 250355, China

Complete contact information is available at:

<https://pubs.acs.org/10.1021/acsomega.4c09799>

Author Contributions

M.Q.: resources, supervision, writing-review and editing. Y.W.: writing-original draft, investigation, formal analysis, conceptualization methodology, writing-review and editing. X.Y.: investigation and project administration. J.Z.: validation and investigation. M.G.: supervision, resources, writing-review and editing.

Funding

This study was supported by the Shandong Provincial Natural Science Foundation of China [grant number ZR2021LZY043].

Notes

All data were generated in-house, and no paper mill was used. All authors agree to be accountable for all aspects of the work, ensuring integrity and accuracy.

The authors declare no competing financial interest.

ABBREVIATIONS

ERK, extracellular regulated protein kinases; GSH-Px, glutathione peroxidase; iNOS, inducible nitric oxide synthase; JNK, c-Jun N-terminal kinase; MAPK, mitogen-activated protein kinase; MDA, malondialdehyde; MITF, microphthalmia-associated transcription factor; NF- κ B, nuclear factor kappa-B; NLRP3, nucleotide-binding oligomerization domain-like receptor protein; Nrf2, nuclear factor erythroid 2-related factor 2; ROS, reactive oxygen species; SOD, superoxide dismutase; TNF- α , tumor necrosis factor-alpha; TRP-1, tyrosinase-related protein-1; TRP-2, tyrosinase-related protein-2; TYR, tyrosinase; UV, ultraviolet radiation

REFERENCES

- (1) (a) Lee, A. Y. Recent progress in melasma pathogenesis. *Pigment Cell Melanoma Res.* **2015**, *28* (6), 648–660. (b) Passeron, T.; Picardo, M. Melasma, a photoaging disorder. *Pigment Cell Melanoma Res* **2018**, *31* (4), 461–465.
- (2) Wirya, S. A.; de Castro Maymone, M. B.; Widjajahakim, R.; Vashi, N. A. Subclinical melasma: Determining disease extent. *J. Am. Acad. Dermatol.* **2017**, *77* (2), No. e41–e42.
- (3) Gauthier, Y.; Cario, M.; Pain, C.; Lepreux, S.; Benzekri, L.; Taieb, A. Oestrogen associated with ultraviolet B irradiation recapitulates the specific melanosome distribution observed in caucasoid melasma. *Br. J. Dermatol.* **2019**, *180* (4), 951–953.
- (4) Lim, H. W.; Kohli, I.; Ruvoilo, E.; Kolbe, L.; Hamzavi, I. H. Impact of visible light on skin health: The role of antioxidants and free radical quenchers in skin protection. *J. Am. Acad. Dermatol.* **2022**, *86* (3s), S27–s37.
- (5) (a) Shike, S.; Yudi, Z.; Rongheng, L. Blood rheology and clinical. *Modern Medical J.* **2017**, *45* (1), 163–167. (b) Lin, X. Y.; Zhou, G. P.; Li, L. A preliminary analysis of serum enzymes and hemorrheology for chloasma in female patients. *J. Clin. Dermatol.* **1997**, No. 6, 359–361.
- (6) (a) Xu, Y.; Tan, H. Y.; Li, S.; Wang, N.; Feng, Y. Panax notoginseng for Inflammation-Related Chronic Diseases: A Review on the Modulations of Multiple Pathways. *Am. J. Chin. Med.* **2018**, *46* (5), 971–996. (b) Xia, L.; Liu, X.; Mao, W.; Guo, Y.; Huang, J.; Hu, Y.; Jin, L.; Liu, X.; Fu, H.; Du, Y.; et al. Panax notoginseng saponins normalises tumour blood vessels by inhibiting EphA2 gene expression to modulate the tumour microenvironment of breast cancer. *Phytomedicine* **2023**, *114* (114), 154787. (c) Zhu, P.; Jiang, W.; He, S.; Zhang, T.; Liao, F.; Liu, D.; An, X.; Huang, X.; Zhou, N. Panax notoginseng saponins promote endothelial progenitor cell angiogenesis via the Wnt/ β -catenin pathway. *BMC Complement. Med. Ther.* **2021**, *21* (1), 53. (d) Huan, C.; Zhou, Z.; Yao, J.; Ni, B.; Gao, S. The Antiviral Effect of Panax Notoginseng Polysaccharides by Inhibiting PRV Adsorption and Replication In Vitro. *Molecules* **2022**, *27* (4), 1254.
- (7) (a) Yin, Z.; Wang, X.; Yang, X.; Chen, Y.; Duan, Y.; Han, J. Salvia miltiorrhiza in Anti-diabetic Angiopathy. *Curr. Mol. Pharmacol.* **2021**, *14* (6), 960–974. (b) Tian, T.; Xu, L. M. [Effects of Salvia miltiorrhiza and salvianolic acid B on microcirculation of liver in mice with portal hypertension]. *Zhong Xi Yi Jie He Xue Bao* **2009**, *7* (2), 151–156.
- (8) (a) Shan, X.-X.; Hong, B.-Z.; Liu, J.; Wang, G.-K.; Chen, W.-D.; Yu, N.-J.; Peng, D.-Y.; Wang, L.; Zhang, C.-Y. [Review of chemical composition, pharmacological effects, and clinical application of Salviae Miltiorrhizae Radix et Rhizoma and prediction of its Q-markers]. *Zhongguo Zhong Yao Za Zhi.* **2021**, *46* (21), 5496–5511. (b) Liu, Y.-Q.; Zhang, R.; Li, W.; Du, H.-Z.; Wu, S.-S.; Xiong, R.; Hou, X.-J.; Zhang, M.; Wang, X.-J. [Study on effects of different habitat processing methods of Salviae Miltiorrhizae Radix et Rhizoma in rats with acute myocardial ischemia]. *Zhongguo Zhong Yao Za Zhi.* **2020**, *45* (23), 5694–5700.
- (9) Yin, S. J.; Luo, Y. Q.; Zhao, C. P.; Chen, H.; Zhong, Z. F.; Wang, S.; Wang, Y. T.; Yang, F. Q. Antithrombotic effect and action mechanism of Salvia miltiorrhiza and Panax notoginseng herbal pair on the zebrafish. *Chin. Med.* **2020**, *15*, 35.
- (10) Hopkins, A. L. Network pharmacology. *Nat. Biotechnol.* **2007**, *25* (10), 1110–1111.
- (11) Barrett, T.; Wilhite, S. E.; Ledoux, P.; Evangelista, C.; Kim, I. F.; Tomashevsky, M.; Marshall, K. A.; Phillippy, K. H.; Sherman, P. M.; et al. NCBI GEO: Archive for functional genomics data sets—update. *Nucleic Acids Res.* **2013**, *41* (Database issue), D991–995.
- (12) Chen, L.; Zhang, Y. H.; Wang, S.; Zhang, Y.; Huang, T.; Cai, Y. D. Prediction and analysis of essential genes using the enrichments of gene ontology and KEGG pathways. *PLoS One* **2017**, *12* (9), No. e0184129.
- (13) (a) Foolad, N.; Shi, V.; Prakash, N.; Kamangar, F.; Sivamani, R. K. The association of the sebum excretion rate with melasma, erythematotelangiectatic rosacea, and rhytides. *Dermatol Online J.* **2015**, *21*, 6. (b) Kleuser, B.; Japtok, L. Sphingolipids and inflammatory diseases of the skin. *Handb. Exp. Pharmacol.* **2013**, *21* (6), 355–372. (c) Flori, E.; Mastrofrancesco, A.; Mosca, S.; Ottaviani, M.; Briganti, S.; Cardinali, G.; Filoni, A.; Cameli, N.; Zaccarini, M.; Zouboulis, C. C.; et al. Sebocytes contribute to melasma onset. *iScience* **2022**, *25* (3), 103871.
- (14) Huang, Y.-D.; Cheng, J.-X.; Shi, Y.; Gao, Z.-H.; Hu, Y.-Y.; Kang, R.; Wang, Y.; Liu, Y.; Ma, S.-C. [Panax notoginseng: A review on chemical components, chromatographic analysis, P. notoginseng extracts, and pharmacology in recent five years]. *Zhongguo Zhong Yao Za Zhi.* **2022**, *47* (10), 2584–2596.
- (15) Zeng, H.; Su, S.; Xiang, X.; Sha, X.; Zhu, Z.; Wang, Y.; Guo, S.; Yan, H.; Qian, D.; Duan, J. Comparative Analysis of the Major Chemical Constituents in Salvia miltiorrhiza Roots, Stems, Leaves and Flowers during Different Growth Periods by UPLC-TQ-MS/MS and HPLC-ELSD Methods. *Molecules* **2017**, *22*, 771.
- (16) McKesey, J.; Tovar-Garza, A.; Pandya, A. G. Melasma Treatment: An Evidence-Based Review. *Am. J. Clin. Dermatol.* **2020**, *21* (2), 173–225.
- (17) (a) Garg, D.; Ng, S. S. M.; Baig, K. M.; Driggers, P.; Segars, J. Progesterone-Mediated Non-Classical Signaling. *Trends Endocrinol. Metab.* **2017**, *28* (9), 656–668. (b) Savouret, J. F.; Chachereau, A.; Misrahi, M.; Lescop, P.; Mantel, A.; Bailly, A.; Milgrom, E. The progesterone receptor. Biological effects of progestins and anti-progestins. *Hum. Reprod.* **1994**, *9*, 7–11.
- (18) Katzenellenbogen, B. S. Mechanisms of action and cross-talk between estrogen receptor and progesterone receptor pathways. *J. Soc. Gynecol. Invest.* **2000**, *7* (1 Suppl), S33–37.
- (19) (a) Jian, D.; Jiang, D.; Su, J.; Chen, W.; Hu, X.; Kuang, Y.; Xie, H.; Li, J.; Chen, X. Diethylstilbestrol enhances melanogenesis via cAMP-PKA-mediated up-regulation of tyrosinase and MITF in mouse B16 melanoma cells. *Steroids* **2011**, *76* (12), 1297–1304. Kim, N. H.; Cheong, K. A.; Lee, T. R.; Lee, A. Y. PDZK1 upregulation in estrogen-related hyperpigmentation in melasma. *J. Invest. Dermatol.* **2012**, *132* (11), 2622–2631. Kippenberger, S.; Loitsch, S.; Solano, F.; Bernd, A.; Kaufmann, R. Quantification of tyrosinase, TRP-1, and Trp-2 transcripts in human melanocytes by reverse transcriptase-competitive multiplex PCR—regulation by steroid hormones. *J. Invest. Dermatol.* **1998**, *110* (4), 364–367.
- (20) Wiedemann, C.; Nägele, U.; Schramm, G.; Berking, C. Inhibitory effects of progestogens on the estrogen stimulation of melanocytes in vitro. *Contraception* **2009**, *80* (3), 292–298.
- (21) Wang, D.; Lu, X.; Wang, E.; Shi, L.; Ma, C.; Tan, X. Salvianolic acid B attenuates oxidative stress-induced injuries in enterocytes by

activating Akt/GSK3 β signaling and preserving mitochondrial function. *Eur. J. Pharmacol.* **2021**, 909, 174408.

(22) Yifan, Z.; Luwei, X.; Kai, L.; Liuhua, Z.; Yuzheng, G.; Ruipeng, J. Protective effect of salvianolic acid B against oxidative injury associated with cystine stone formation. *Urolithiasis* **2019**, 47 (6), 503–510.

(23) Lin, Z.; Bao, Y.; Hong, B.; Wang, Y.; Zhang, X.; Wu, Y. Salvianolic acid B attenuated cisplatin-induced cardiac injury and oxidative stress via modulating Nrf2 signal pathway. *J. Toxicol. Sci.* **2021**, 46 (5), 199–207.

(24) Zhang, Z.; Ji, J.; Zhang, D.; Ma, M.; Sun, L. Protective effects and potential mechanism of salvianolic acid B on sodium laurate-induced thromboangiitis obliterans in rats. *Phytomedicine* **2020**, 66, 153110.

(25) Zhao, Y.; Shao, C.; Zhou, H.; Yu, L.; Bao, Y.; Mao, Q.; Yang, J.; Wan, H. Salvianolic acid B inhibits atherosclerosis and TNF- α -induced inflammation by regulating NF- κ B/NLRP3 signaling pathway. *Phytomedicine* **2023**, 119, 155002.

(26) Wells, P. G.; Kim, P. M.; Laposa, R. R.; Nicol, C. J.; Parman, T.; Winn, L. M. Oxidative damage in chemical teratogenesis. *Mutat. Res.* **1997**, 396 (1–2), 65–78.

(27) Seçkin, H. Y.; Kalkan, G.; Baş, Y.; Akbaş, A.; Önder, Y.; Özyurt, H.; Sahin, M. Oxidative stress status in patients with melasma. *Cutan Ocul Toxicol.* **2014**, 33 (3), 212–217.

(28) (a) Liu, W.; Chen, Q.; Xia, Y. New Mechanistic Insights of Melasma. *Clin. Cosmet. Investig. Dermatol.* **2023**, 16, 429–442. (b) Gu, Y.; Han, J.; Jiang, C.; Zhang, Y. Biomarkers, oxidative stress and autophagy in skin aging. *Ageing Res. Rev.* **2020**, 59, 101036. (c) Artzi, O.; Horovitz, T.; Bar-Ilan, E.; Shehadeh, W.; Koren, A.; Zusmanovitch, L.; Mehrabi, J. N.; Salameh, F.; Isman Nelkenbaum, G.; Zur, E.; et al. The pathogenesis of melasma and implications for treatment. *J. Cosmet. Dermatol.* **2021**, 20 (11), 3432–3445. (d) Li, W.; Xing, Q.; Liu, Z.; Liu, R.; Hu, Y.; Yan, Q.; Liu, X.; Zhang, J. The signaling pathways of traditional Chinese medicine in treating diabetic retinopathy. *Front. Pharmacol.* **2023**, 14, 1165649.